Available online at www.sciencedirect.com
SCIENCE DIRECT®
Journal of Solid State Chemistry 177 (2004) 1624–1630
JOURNAL OF SOLID STATE CHEMISTRY
http://elsevier.com/locate/jssc

Synthesis of ktenasite, a double hydroxide of zinc and copper, and its intercalation reaction

Mei Xue,[a,*] Ramesh Chitrakar,[a] Kohji Sakane,[a] Kenta Ooi,[a] Shoichi Kobayashi,[b] Masayuki Ohnishi,[b] and Akira Doi[c]

[a] *Institute for Marine Resources and Environment, National Institute for Advanced Science and Technology, AIST-Shikoku, 2217-14 Hayashi-cho, Takamatsu 761-0395, Japan*

[b] *Department of Chemistry and Bioscience, College of Science and Industrial Technology, Kurashiki University of Science and the Arts, Kurashiki 712-8505, Japan*

[c] *Department of Applied Art, College of Science and Industrial Technology, Kurashiki University of Science and the Arts, Kurashiki 712-8505, Japan*

Received 7 September 2003; received in revised form 25 November 2003; accepted 14 December 2003

Abstract

Ktenasite was synthesized by the simple method of mixing ZnO powder with $CuSO_4$ solution at room temperature. The X-ray diffraction pattern of synthesized ktenasite was very similar to that of mineral ktenasite. The lattice parameters were determined as $a = 0.559$, $b = 0.616$, $c = 2.374$ nm and $\beta = 95.63°$, which agreed comparatively well with those for mineral ktenasite. The synthesized ktenasite consisted of thin rectangular particles ranging in size from 2 to 4 μm in length. TEM observation suggested the formation of a super lattice structure in the *a*-axis direction and significant crystal growth in the *b*-axis direction. The intercalation reaction of sodium dodecyl sulfate (NaDS) with ktenasite showed that the intercalation took place accompanied by the expansion of basal spacing from 1.17 to 2.70 nm. The reaction progressed by the SO_4^{2-}/DS^- anion exchange mechanism with the dissolution of interlayer $[Zn(H_2O)_6]SO_4$ salt.

Keywords: Ktenasite; Intercalation; Anion-exchange

1. Introduction

The mineral ktenasite was first reported by Kokkoros in 1950 as a basic copper zinc sulfate with the proposed formula as $(Cu,Zn)_3SO_4(OH)_4 2H_2O$ occurring at Kamariza Mine (Greece) [1]. Raade et al. [2] found a green, plate-like mineral in Glomsrudkollen zinc mine (Norway) and, using X-ray powder data described it in detail, as a monoclinic, space group $P2_1/c$ with lattice parameters $a = 0.559$, $b = 0.612$, $c = 2.376$ nm, $\beta = 95.55°$ and the chemical formula $(Cu_{3.5}Zn_{1.5})(SO_4)_2(OH)_6 \cdot 6H_2O$. Different authors have since reported ktenasite in Italy, USA, Germany [3–5]. Recently, Ohnishi et al. [6] found ktenasite in Hirano mine (Japan).

The reaction of a solid oxide with aqueous metal solutions to prepare hydroxy double salts has been known for a long time [7,8]. Lagaly et al. [9] prepared a series of hydroxy double salts (nitrate) of Zn, Cu, Co, Ni, etc. For instance, ZnO dispersed in $Cu(NO_3)_2$ solution at 65°C for 3 days transforms into $ZnCu_{1.5}(NO_3)_{1.13}(OH)_{3.88}$ with a basal spacing of 0.7 nm. These authors proposed that hydroxy double salts comprise a class of layered compounds which are similar to hydrotalcite-like compounds and show anion exchange properties. Yamanaka et al. [10,11] and other researchers [12–14] have prepared layered double hydroxide salts of certain divalent metals such as Ni–Zn and Zn–Cu and have shown to undergo anion exchange reactions.

There has been no report on the synthesis of ktenasite in the literature. The double hydroxide salt of Zn^{2+} and Cu^{2+} reported by Lagaly et al. [9] does not represent ktenasite. In the present paper, we prepared ktenasite by mixing ZnO with $CuSO_4$ solution at room temperature.

*Corresponding author. Fax: +81-87-869-3551.
E-mail addresses: xue-mei@aist.go.jp (M. Xue), k-ooi@aist.go.jp (K. Ooi).

0022-4596/$ - see front matter © 2004 Elsevier Inc. All rights reserved.
doi:10.1016/j.jssc.2003.12.026

We also studied the intercalation reaction of sodium dodecyl sulfate (NaDS) into ktenasite.

2. Experimental

2.1. Preparation

Ktenasite was prepared by a chemical reaction using a $CuSO_4$ solution and ZnO powder. The chemicals used in the synthesis were purchased and used without further purification. ZnO powder (2 g) was added to 50 cm^3 of 0.64 M (1 M = 1 mol/dm^3) $CuSO_4$ aqueous solution (Cu/Zn mole ratio = 1.25) under vigorous stirring at room temperature for 2 h. After stirring, the precipitate was aged at room temperature for 1 d, then separated by centrifugation, washed with water and finally dried at room temperature for 2 d. Initial and final pH values during the preparation were 3.4 and 5.3, respectively. The color of the resultant ktenasite was bluish green.

2.2. Anion-exchange reaction

Ktenasite (0.1 g) was mixed with a 0.01 M sodium dodecyl sulfate $CH_3(CH_2)_{11}OSO_3Na$ (NaDS) solution (100 cm^3). The mole amount of NaDS added was 4 times that of the sulfate content of ktenasite. After equilibrating for 1 d at room temperature, the solid was separated by filtration and air-dried. The total carbon content of the DS-exchanged solid was determined by a Sumigraph-type NCH-21 carbon analyzer.

2.3. Characterization

X-ray diffraction analysis was carried out using a Rigaku type RINT 1200 X-ray diffractometer with Ni-filtered Cu$K\alpha$ radiation ($\lambda = 1.5404$ Å) and graphite monochromator. The data were collected at room temperature in the range of 2θ between 2° and 40°. Lattice parameters were refined by the least square method. Infrared spectra were obtained by the KBr method on a Perkin-Elmer infrared spectrometer (1600 Series FTIR). The TG–DTA curve was measured on a MAC Science Thermal Analyzer (System 001, TG–DTA 2000) at a heating rate of 10°C/min in air. SEM and TEM observations were carried out on a Hitachi-type S-2460 N scanning electron microscope and JEOL-type JEM-3010 transmission electron microscope, respectively.

2.4. Chemical analysis

After synthesized ktenasite (50 mg) was dissolved in a 0.5 M HCl solution, the Cu and Zn contents were determined with a Shimadzu AA-760 atomic absorption spectrophotometer. The SO_4 content was determined by gravimetric method after precipitation with a $BaCl_2$ solution.

3. Results and discussion

3.1. Chemical composition of ktenasite

During mixing of solid ZnO (2.0 g) with 50 mL of 0.64 M $CuSO_4$ solution, the dissolution/precipitation reactions occur, enhancing the crystallization of the ktenasite. The chemical formula, calculated from the metal ion contents, SO_4 content, and the water content determined from the weight loss by heating at 300°C, is given in Table 1. The hydroxide content was calculated on the basis of the condition of electrical neutrality. The Cu/Zn molar ratio of the starting reaction solution was 1.25 and that of the solid product was 3.0. The difference in Cu/Zn ratio can be attributed to the dissolution of 63% of Zn from solid ZnO during the formation of ktenasite. The composition of synthesized ktenasite was close to that observed for

Table 1
Chemical analysis and lattice parameters of synthesized ktenasite

	Mineral ktenasite[8]	Synthesized ktenasite
Lattice parameter (nm)	$a_0 = 0.559$ $b_0 = 0.616$ $c_0 = 2.374$ $\beta = 95.63°$	$a_0 = 0.562$ $b_0 = 0.610$ $c_0 = 2.39$ $\beta = 95.3°$
Weight (%)	CuO 37.87 ZnO 16.31 CoO 0.83 PbO 0.54 NiO 0.07 SO_3 22.15 H_2O 22.38	CuO 41.7 ZnO 14.3 CoO — PbO — NiO — SO_3 21.6 H_2O 21.1
Chemical formula	$Cu_{3.45}Zn_{1.45}Co_{0.08}Pb_{0.02}Ni_{0.007}(SO_4)_2(OH)_{5.99} \cdot 5.99H_2O$	$Cu_{3.88}Zn_{1.28}(SO_4)_2(OH)_{6.32} \cdot 6.24H_2O$

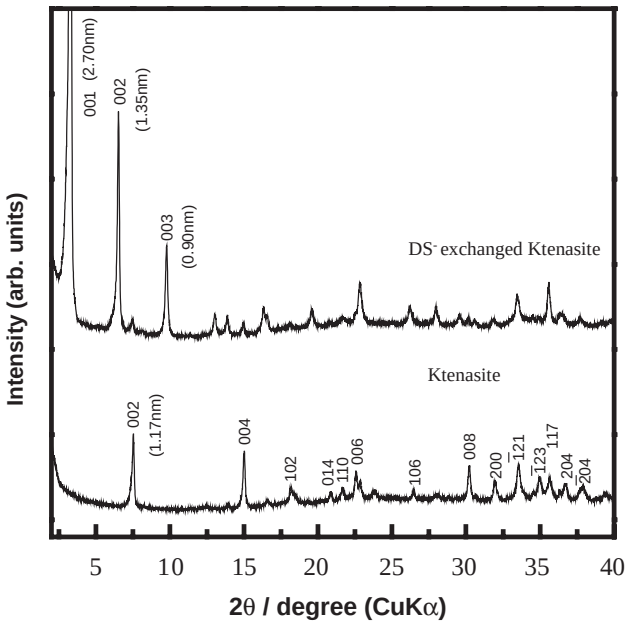

Fig. 1. X-ray diffraction patterns of ktenasite and NaDS-exchanged ktenasite.

mineral ktenasite [4]. On the basis of the model [4], the chemical formula of the present sample can be written as $\{(Cu_{3.88}Zn_{0.78})(OH)_{6.32}\}^{3+}(SO_4)_2^{4-}$ $[Zn(H_2O)_6]_{0.5}^{2+}\cdot 0.24H_2O$, where $\{(Cu_{3.88}Zn_{0.78})(OH)_{6.32}\}^{3+}$ represents the octahedral Cu–Zn sheet and $[Zn(H_2O)_6]^{2+}$ represents the interlayer Zn ions. The SO_4^{2-} ions are located between the octahedral sheets and the interlayer Zn^{2+} ions.

3.2. X-ray diffraction analysis

The XRD pattern of the synthesized ktenasite is shown in Fig. 1 (bottom). The diffraction peaks can be indexed to the monoclinic structure of ktenasite mineral with the chemical formula $(CuZn)_5(SO_4)_2(OH)_6$ (JCPDS No. 29-0591). Indexed peaks of synthesized ktenasite and ktenasite mineral JCPDS (29-0591) are included in Table 2. The main peaks of the synthesized ktenasite (I_{002}, I_{004}, I_{102}) are comparable to those of ktenasite mineral reported in the literature [6]. The lattice parameters of the synthesized ktenasite are given in Table 1, along with data from mineral ktenasite for comparison. Mellini and Merlino [4] determined the crystal structure for ktenasite from Minieera (Italy). The structure is characterized by corrugated sheets of distorted copper–zinc polyhedra and sulfate groups are connected to both sides of the octahedral sheets by corner sharing. The Zn cation in the octahedral site coordinates with six water molecules, which are connected to the oxygen atom of the sulfate group through hydrogen bonding (Fig. 2).

3.3. DTA–TG analysis

The DTA–TG curve of ktenasite is shown in Fig. 3 (left). A small endothermic peak around 79°C is due to the dissipation of water adsorbed on the surface of ktenasite. A sharp endothermic peak around 140°C is due to the loss of interlayer water, most of which is coordinated to the interlayer Zn^{2+} ions to form $[Zn(H_2O)_6]^{2+}$ cations. Two small endothermic peaks around 200°C and 324°C are due to the condensation of hydroxyl groups of the copper and zinc layers, accompanied by the dissipation of water molecules. Since $ZnSO_4$ and $CuSO_4$ transform into ZnO and CuO with an evolution of SO_3 gas at around 730°C and 820°C, respectively [15], the endothermic peaks at 728°C and 815°C can be assigned to the destruction of sulfate with the dissipation of SO_3 gas to form ZnO and CuO, respectively. The weight loss (20.4%) between 600°C and 830°C is close to the SO_3 content calculated from the chemical analysis result. An unidentified exothermic peak without weight loss is observed at 522°C, probably due to the structural transformation of metal sulfate oxide.

3.4. FT-IR analysis

The infrared spectrum (IR) of ktenasite was measured by the KBr method in the region 4000–400 cm^{-1}, as shown in Fig. 4 (bottom). The sharp peaks at 3579, 3521, and 3429 cm^{-1} can be assigned to hydrogen bonding modes $\nu(O-H\cdots O)$ of the hydroxyl groups of the octahedral sheet. This suggests the presence of

different kinds of hydrogen bonding in the ktenasite. These peaks can be assigned to the vibration of hydroxide groups of the Cu–Zn octahedral sheet. A broad band around 3150 cm^{-1} and a relatively sharp band at 1617 cm^{-1} are due to the stretching and bending vibrations of the crystal water. Absorption bands in the region 1000–1200 cm^{-1} are attributed to the vibrations of the SO_4 group [2]. The bands below 1000 cm^{-1} are due to the vibrations by the lattice of copper and zinc octahedra.

Table 2
Comparison of X-ray powder diffraction data for ktenasite material and ktenasite mineral JCPDS 29-0591

h k l	Ktenasite mineral (JCPDS 29-0591)		Ktenasite material	
	d (Å)	*I*	*d* (Å)	*I*
0 0 2	11.820	100	11.872	100
—	—	—	7.143[a]	12
—	—	—	6.393[a]	15
0 0 4	5.910	85	5.933	87
0 1 1	5.930			
0 1 2	5.440	5	5.368	18
1 0 2	4.850	90	4.907	35
—	—	—	4.833[a]	27
−1 0 4	4.260	15	4.275	23
1 1 0	4.120	30	4.118	26
1 1 1	4.020	10	—	—
0 0 6	3.947	20	3.955	41
1 0 4	3.881	10	3.904	31
−1 1 3	3.754	20	3.751	21
−1 0 6	3.377	15	3.378	20
−1 1 5	3.227	5	3.195	17
1 0 6	3.083	10	3.106	15
0 2 0	3.067	10	3.046	13
0 0 8	2.955	50	2.965	41
−1 1 6	2.955			
2 0 0	2.785	60	2.804	28
−1 2 1	2.690	60	2.675	40
1 2 0	2.688			
2 0 2	2.655	50	—	—
−2 0 4	2.620	5	—	—
—	—	—	2.603[a]	18
−1 2 3	2.59	70	2.572	30
1 2 2	2.584			
−2 1 0	2.535	10	—	—
1 1 7	2.530	5	2.523	29
2 1 1	2.496	10	—	—
2 0 4	2.433	20	2.452	26
−2 1 4	2.409	5	—	—
−2 0 6	2.385	40	2.375	23
−2 1 5	2.320	5	—	—

[a] Unknown peak.

3.5. SEM and TEM photographs

The crystal morphology of ktenasite was observed in the SEM images (Fig. 5 top left). It consists of thin rectangular particles ranging in size from 2 to 4 μm in length. The crystallite size was about 30 nm estimated by the widths of 002 peak in ktenasite. The TEM image of crystal particles (left) and the corresponding selected area diffraction (SAD) pattern (right) is shown in Fig. 6. The satellite spot shown in the figure was observed between {200} and {300} reflection, which may be due to the presence of vacancy in the Cu(1) and Cu(2) sites of distorted octahedral sheets. The satellite spots suggests that there is twice the periodicity of unit cells with super lattice structure in the *a*-axis direction and crystal growth is significant in the *b*-axis direction.

3.6. Characterization of NaDS treated ktenasite

The XRD pattern of NaDS-exchanged ktenasite is shown in Fig. 1 (top). Intercalation of NaDS in ktenasite results in an expansion of the layers with an increase in basal spacing from 1.17 to 2.70 nm. The I_{001} peak is sharp and strong; its intensity is markedly higher than the I_{002} peak of the ktenasite. This indicates that the layered sheets of the NaDS-treated sample are stacked in orderly manner. Intercalation of NaDS to hydrotalcite-like materials also showed an expansion of the basal spacing to 2.52 nm [16–18]. The high crystallinity obtained in the present NaDS-exchanged ktenasite may be attributed to the self-organization of DS anions in the interlayer domains. In ktenasite, $[Zn(H_2O)_6]_{0.5}^{2+}$ cations are connected to the oxygen atoms of sulfate

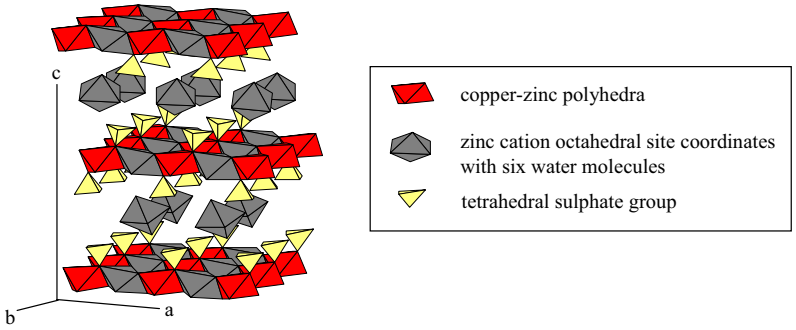

Fig. 2. Schematic structure of ktenasite.

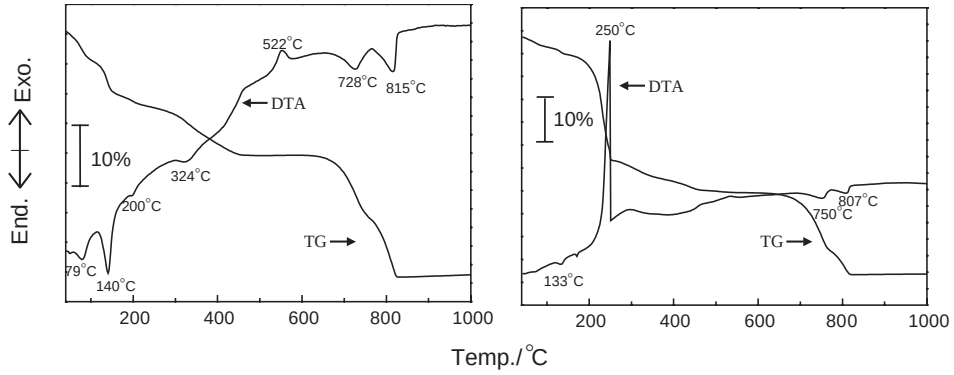

Fig. 3. DTA–TG curves of ktenasite and NaDS-exchanged ktenasite (heating in air, 10°C/min).

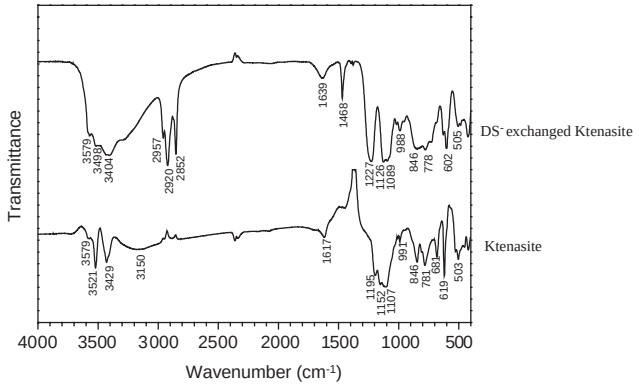

Fig. 4. FT-IR spectra of ktenasite and NaDS-exchanged ktenasite.

groups through hydrogen bonding and the sulfate groups are also directly linked to the Cu–Zn octahedral sheets. After the DS^- exchange with sulfate groups in ktenasite, the cleavage of hydrogen bond occurs resulting in the dissolution of zinc ions and the DS^- groups are directly linked with the octahedral sheets of Cu–Zn and no other cations are inserted between the subsequent layers. The dissolution of Zn was ca. 40%, that coincides with the results of mineral ktenasite in which 40% of Zn are distributed in $[Zn(H_2O)_6]^{2+}$ present in the interlayer space and 60% of Zn are distributed in the Cu(1) and Cu(2) sites of octahedral sheets [4]. Since the interlayer $[Zn(H_2O)_6]^{2+}$ ions may dissolve as sulfate salt, the chemical formula after the dissolution can be written hypothetically as $\{(Cu_{3.88}Zn_{0.78})(OH)_{6.32}\}^{3+}\}(SO_4)^{3-}_{1.5}\cdot 0.24H_2O$.

From the chemical analysis, the total carbon content was 16.8%; this shows that the amount of DS anion intercalated is 1.17 mmol/g. Since the DS-exchanged phase did not contain Na^+ ions, only anion exchange intercalation occurs with ktenasite. The chemical analysis of the DS^- intercalated sample showed an increase of the Cu/Zn mole ratio to 5.7 as compared with a Cu/Zn ratio of 3.0 in the original ktenasite. The amount of Zn dissolved, determined from the Zn concentration in the supernatant solution, was 0.71 mmol/g. This indicates that the intercalation reaction progresses as a SO_4^{2-}/DS^- anion exchange reaction with the dissolution of interlayer $[Zn(H_2O)_6]^{2+}$ ions.

The exact composition of DS-exchanged ktenasite was calculated from the chemical analysis of Zn, Cu, DS^- ions, SO_3, and water contents. The water content was determined from the weight loss by the heating at 200°C. The composition was $Cu_{3.88}Zn_{0.68}(OH)_{7.4}[CH_3(CH_2)_{11}SO_4]_{0.87}(SO_4)_{0.42}\cdot 2.0H_2O$. This suggests that octahedral sheets of copper and zinc hydroxide are maintained and the intercalation of DS^- ions progresses by the ion exchange with the residual sulfate ions in the interlayer. The electrical neutrality on DS-exchanged ktenasite is maintained by the exchange of DS^- groups with equivalent amount of sulfate ions. We can conclude from these calculations that both the dissolution of interlayer zinc ions as zinc sulfate salt and the SO_4^{2-}/DS^- ion exchange reaction progress simultaneously during the DS^- intercalation, maintaining the electro-neutrality.

The DTA–TG curve of the NaDS-exchanged phase is shown in Fig. 3 (right). The endothermic peak around 140°C was weakened markedly by the DS intercalation, due to the removal of the interlayer crystal water as $Zn(H_2O)_6^{2+}$ ions. A sharp exothermic peak at 250°C with accompanying weight loss (22%) was due to the decomposition of DS^- in the interlayer as carbon dioxide and water. The weight loss agreed comparatively well with the hydrocarbon content (20%) calculated from the total carbon content. Small endothermic peaks around 750°C and 807°C are due to the destruction of sulfate with the dissipation of SO_3 gas, similar to the case of starting ktenasite. The SO_3 content calculated from the weight loss is 2.24 mmol/g; this shows that a considerable amount (1.7 mmol/g) of SO_4^{2-} remains even after the DS intercalation.

The infrared spectrum (IR) of NaDS-exchanged ktenasite is shown in Fig. 4 (top). The sharp peaks around 3400, 3500, and 3600 cm^{-1} remained after the intercalation reaction, while the broad band around

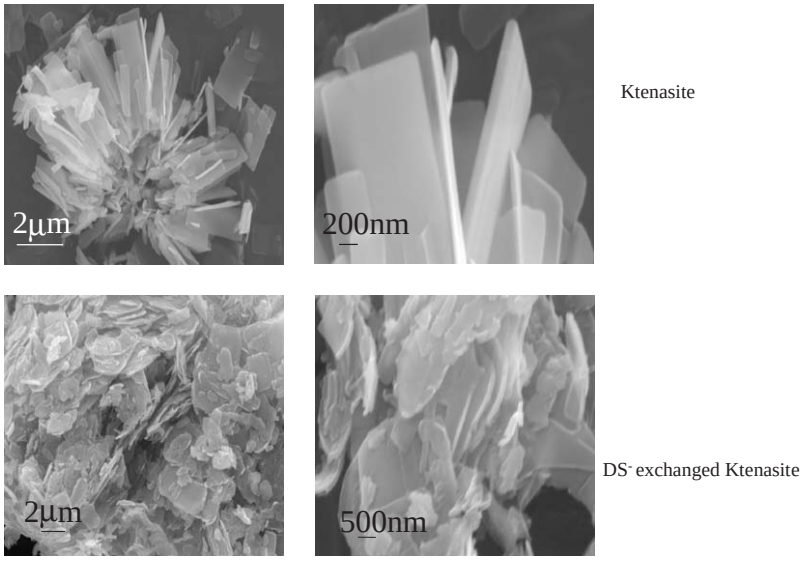

Fig. 5. SEM images of ktenasite and NaDS-exchanged ktenasite.

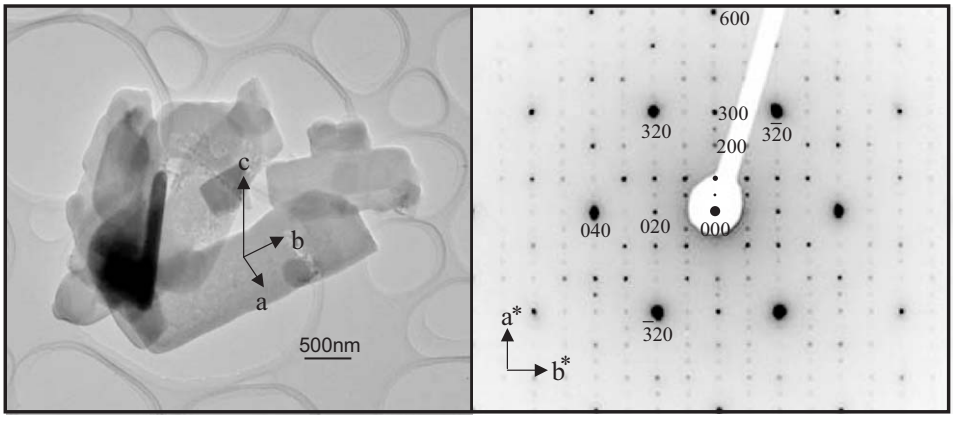

Fig. 6. TEM image and corresponding SAD pattern of ktenasite.

3150 cm^{-1} disappeared. This also shows that the hydroxide group of octahedral sheet remains, while the interlayer crystal water is removed by the intercalation of DS^- anions. The sharp bands at 2957, 2920 and 2852 cm^{-1} are due to the C–H stretching vibrations. The assignment for the absorption band at 1639 cm^{-1} was due to bending mode of the adsorbed water molecules. It contains a small amount of water molecules. Sharp peaks at 1468 and 1227 cm^{-1} can be ascribed to the C–H bending vibrations and C–H twist vibrations, respectively. Bands around 1050–1150 cm^{-1}, attributed to the vibrations of SO_4 group, do not change markedly by the DS^- intercalation, due to the remaining SO_4^{2-} as well as to the intercalation of the R–O–SO_3 group.

NaDS-exchanged ktenasite did not retain its angular form; instead well-developed platelets formed (Fig. 5 right). The crystallite size was about 30 nm estimated by the widths of 001, 002 peaks in DS-exchanged ktenasite using Debye-Scherrer equation. A small portion of metal hydroxide dissolution may take place at the corners of rectangular sheets.

3.7. Mechanism of DS^- intercalation

Since ktenasite contains both the anion (SO_4^{2-}) and cation ($[Zn(H_2O)_6]^{2+}$) in the interlayer between oxide sheets, the intercalation reaction is different from that of a hydrotalcite-like compound where a simple exchange reaction of charge-compensating anions in the interlayer takes place. On the basis of the above results, the intercalation reactions can be written schematically as shown in Fig. 7. The intercalation reaction progresses by the SO_4^{2-}/DS^- anion exchange mechanism with a dissolution of interlayer $[Zn(H_2O)_6]SO_4$ salt. Since the length of the hydrocarbon group of DS^- is 2.08 nm [16], the interlayer DS^- may arrange itself nearly perpendicular to the hydroxide sheets to form one molecular layer of DS^- in the interlayer. Clearfield et al. [19]

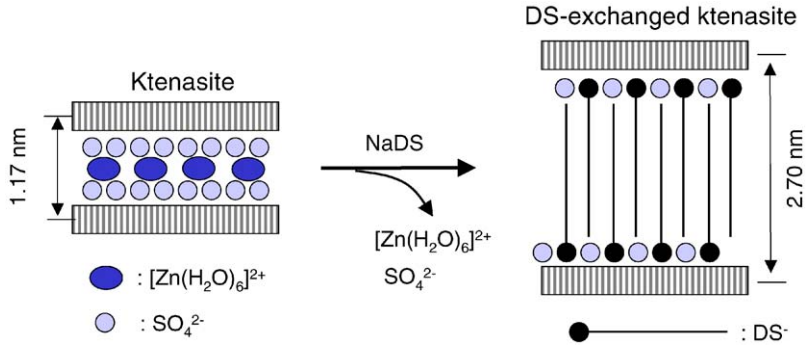

Fig. 7. Schematic representation of DS^- intercalation into ktenasite.

showed the incorporation of DS^- intercalation into a series of Ni–Al, Mg–Al and Zn–Cr LDHs and they reported three different gallery heights: 2.6, 3.6 and 4.7 nm. The different basal spacings obtained revealed the existence of three different interlayer anion arrangements, with the shortest (2.6 nm) assigned to perpendicular monolayer arrangement. The interlayer spacing of 3.6 nm was attributed to a bilayer arrangement, in which the anion is tilted at an angle of 40° to the hydroxide layer. The 4.7 nm spacing was considered consistent with a vertical end-to-end bilayer arrangement. In our present study, the gallery height obtained (2.7 nm) is in agreement with a monolayer of DS anions oriented perpendicular to the layers in the interlamellar domain. The implied angle (or tilt angle) between hydrocarbon chain and the layers in DS-exchanged ktenasite material was calculated according to Kopka et al. [20]. The observed basal spacing is slightly larger than the spacing for monolayer perpendicular alkyl sulfate ions and the tilt angle was ca. 90°. A similar study has been reported for Zn–Cr hydroxide layers.

4. Conclusion

Ktenasite with a well-developed plate-like morphology can be prepared by a simple reaction with ZnO and $CuSO_4$. Ktenasite has a unique rectangular morphology with particle size ranging from 2 to 4 μm in length. Ktenasite has a unique structure with both the tetrahedral sulfate anions and octahedral $[Zn(H_2O)_6]^{2+}$ in the interlayer between hydroxide sheets. The intercalation of DS^- results in the expansion of the layer. It progresses by an anion-exchange mechanism with the dissolution of interlayer zinc sulfate.

Acknowledgments

We are grateful to Prof. Yasuhiro Yokota of Okayama University of Science, Japan for providing facilities for TEM measurements.

References

[1] P. Kokkoros, Tschemarks Mineral. Petrogr. Mitt. 1 (1950) 342.
[2] G. Raade, C.J. Elliott, E.E. Fejer, Mineral. Mag. 41 (1977) 65.
[3] J.B. Rankin Jr., Rocks Miner. 44 (1969) 594.
[4] M. Mellini, S. Merlino, Z. Kristallogr. 147 (1978) 129.
[5] A. Livingstone, J. Russell Soc. 4 (1991) 13.
[6] M. Ohnishi, S. Kobayashi, I. Kusachi, J. Mineral. Petrol. Sci. 97 (2002) 185.
[7] A.C.R. Recoura, Hebd. Seances Acad. Sci. 132 (1901) 1414.
[8] O.C.R. Sabatier, Hebd. Seances Acad. Sci. 132 (1901) 1538.
[9] M. Meyn, K. Beneke, G. Lagaly, Inorg. Chem. 32 (1993) 1209.
[10] S. Yamanaka, T. Sato, M. Hattori, Chem. Lett. (1989) 1869.
[11] S. Yamanaka, T. Sato, K. Seki, M. Hattori, Solid State Ionics 53–56 (1992) 527.
[12] W. Nowacki, R. Scheidegger, Helv. Chim. Acta 35 (1952) 375.
[13] W. Stahlin, H.R. Oswald, J. Solid State Chem. 3 (1971) 256.
[14] H. Morioka, H. Tagaya, M. Karasu, J. Kadokawa, K. Chiba, J. Mater. Res. 13 (1998) 848.
[15] G. Liptay, Atlas of Thermal Analytical Curves, Heyden & Son Ltd., London, 1971, pp. 24, 27.
[16] M. Adachi Pagano, C. Forano, J.-P. Besse, Chem. Commun. (2000) 91.
[17] E.L. Crepaldi, P.C. Pavan, J.B. Valim, J. Mater. Chem. 10 (2000) 1337.
[18] F. Leroux, M. Adachi Pagano, M. Intissar, S. Chauviere, C. Forano, J.P. Besse, J. Mater. Chem. 11 (2001) 105.
[19] A. Clearfield, M. Kieke, J. Kwan, J.L. Colon, R.C. Wang, J. Inclusion Phenom. Mol. Recognit. Chem. 11 (1991) 361.
[20] H. Kopka, K. Beneke, G. Lagly, J. Colloid Interface Sci. 123 (1988) 427.